J Electr Eng Technol.2015; 10(3): 709-718
http://dx.doi.org/10.5370/JEET.2015.10.3.709

ISSN(Print) 1975-0102
ISSN(Online) 2093-7423

Flexible Transmission Expansion Planning for Integrating Wind Power Based on Wind Power Distribution Characteristics

Jianxue Wang†, Ruogu Wang*, Pingliang Zeng, Shutang You*, Yunhao Li* and Yao Zhang***

Abstract – Traditional transmission planning usually caters for rated wind power output. Due to the low occurrence probability of nominal capacity of wind power and huge investment in transmission, these planning methods will leads to low utilization rates of transmission lines and poor economic efficiency. This paper provides a novel transmission expansion planning method for integrating large-scale wind power. The wind power distribution characteristics of large-scale wind power output and its impact on transmission planning are analyzed. Based on the wind power distribution characteristics, this paper proposes a flexible and economic transmission planning model which saves substantial transmission investment through spilling a small amount of peak output of wind power. A methodology based on Benders decomposition is used to solve the model. The applicability and effectiveness of the model and algorithm are verified through a numerical case.

Keywords: Large-scale wind power, Wind power distribution characteristics, Transmission planning, Benders decomposition

1. Introduction

Large-scale wind farms usually locate in areas with rich wind resources, low local load levels, and weak electrical networks. To maximize the utilization of wind power, full absorption of wind power policy is always applied to construct the long-distance transmission network for delivering large-scale wind power to load centers, requiring a huge amount of investment [1], such as in China. Therefore, it is necessary to find a flexible and reasonable transmission planning method to deal with large-scale wind power integration.

Generally, transmission planning can be conducted through generation-transmission coordinated planning [2, 3] or performed separately [4, 5]. Some traditional transmission planning methods are based on system reliability and designed to meet demand and reliability requirements [6, 7]. But transmission planning methods for integrating wind power should be different, because wind power does not significantly improve system reliability [8]. In [5], social welfare is considered for evaluating transmission expansion planning. To maximize the benefits of wind power, planning methods are usually based on ensuring the wind power output [9]. However, as wind power is characterized as having a low probability of reaching or approaching its nominal capacity, the transmission construction plan that is designed to cater for rated wind power capacity will lead to the low utilization rate of transmission lines. Especially for cases of large-scale wind power, it could easily lead to investment waste. Besides, since the expansion of network includes not only the construction of lines between wind farms and access points, but also the reinforcement of the existing network, the efficiency of the planning scheme will further reduce. In addition, spilling a reasonable amount of wind under certain circumstances is found to be more economical in system operation with a high level of wind power [10, 11].

Since wind power is developing fast in recent years, facilitating the grid connection of large-scale renewable power has become an urgent task. This paper concentrates on flexible and economic transmission planning for integrating large-scale wind power based on wind power distribution characteristics. The remaining of this paper is organized as follows. Section II analyzes the wind power distribution characteristics of wind power output and its effect on transmission planning. In Section III, the paper proposes a novel transmission planning method for large-scale wind power by considering curtailing a proper amount of peak output of wind power to substantially save transmission investment. The solving procedures through Benders decomposition approach are also provided in Section III. Section IV gives a numerical example to verify the effectiveness of the proposed model and solution method, as well as the sensitivity of the model on parameters. The conclusions are reached in Section V.

2. Wind Power Distribution Characteristics of Wind Output

Wind power output mainly depends on wind speed and wind turbine generator (WTG) characteristics. The former

† Corresponding Author: School of Electrical Engineering, Xian Jiaotong University, China. (jxwang@mail.xjtu.edu.cn)
* School of Electrical Engineering, Xian Jiantong University, China.
** China Electrical Power Research Institute, China.
Received: January 20, 2014; Accepted: November 4, 2014

is considered obeying Weibull distribution [12], and the latter is a piecewise function of wind speed [13] as shown in (1).

$$P_w = \begin{cases} 0 & 0 \le V_w \le V_{ci} \text{ or } V_w \ge V_{co} \\ (\alpha_1 + \alpha_2 \cdot V_w + \alpha_3 \cdot V_w^2) \cdot P_r & V_{ci} \le V_w \le V_r \\ P_r & V_r \le V_w \le V_{co} \end{cases} \quad (1)$$

where P_w and P_r represent actual power output and rated power output, respectively. V_w, V_{ci}, V_r, and V_{co} are actual wind speed, cut-in wind speed, rated wind speed, and cut-out wind speed, respectively. α_1, α_2, and α_3 are coefficients.

In Fig. 1, the dashed curve denotes a typical output characteristic of WTG as described in (1), and the solid curve represents a typical probability distribution of wind speed.

As shown in Fig. 1, this WTG output reaches the rated power only when wind speed is greater than 15m/s. However, according to the wind speed distribution curve, the probability that WTG's output reaches the rated power is very low. Furthermore, the situation that output reaches 70% of rated power also has a low probability of occurring.

To further show the wind power distribution characteristics, Fig. 2 gives the cumulative probability curve of a large-scale wind power base's output in northwest China.

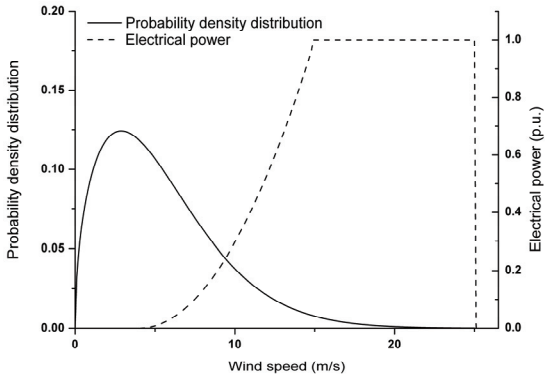

Fig. 1. Wind speed distribution and WTG output characteristics

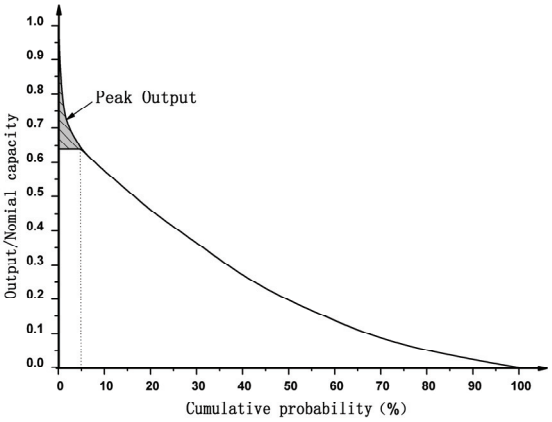

Fig. 2. Cumulative probability curve of a wind power base's output

The cumulative probability curve in Fig. 2 shows that there is a 95% probability that the output is lower than 65% of rated power, with only a 5% probability higher than that. Thus the high level output of the wind power base forms a peak in cumulative probability curve, which is represented by the shaded part in Fig. 2.

In summary, both theories and data statistics [14, 15] prove that for a large wind farm and large-scale wind power bases, the wind power output usually stays in a relatively low level whereas the high level output rarely occurs, thus forming a significant peak in the cumulative probability curve. This characteristic derives from wind speed distribution and WTG characteristics and it is one of the most important distribution characteristics for wind power output.

Energy storage is potential approach to improve this unfavorable characteristic of wind power output. However, a huge amount of storage is needed for large-scale wind power, which is economically infeasible due to the high investment cost. Consequently, in order to ensure full utilization of wind resource, most current transmission plans for wind power cater to the nominal capacity of wind farms. However, as shown in Fig. 2, if the transmission planning caters to the nominal wind power capacity, there would be a 95% probability that the utilization rate of the lines stays below 65%. In other words, 35% of transmission lines are invested specifically for the peak output of wind power, which has a small probability (5%) of occurring.

In fact, sacrificing the line utilization rate to ensure the full transmission of wind power is very uneconomical. If the peak output is curtailed appropriately in planning, the resulting plan will significantly save the investment in building new transmission lines and improve line utilization rates as well [16], while the total cost of wind power loss is relatively small.

Therefore, in the transmission planning for integrating large-scale wind power, saving the investment in new lines and minimizing the cost of wind power curtailment should be both considered, but the two parts are inherently contradictory. In order to find an economical and reasonable planning scheme, an optimum point should be reached to balance the two parts through curtailing a proper amount of wind power output.

3. Transmission Expansion Planning Model for Integrating Wind Power

3.1 The Multi-scenario transmission planning model considering wind power distribution characteristics

3.1.1 Objective function:

The expectation value model is used to handle the

uncertainty characteristic of the wind power output in the transmission planning model [17]. The expected value of wind power output reflects the output level and the probability simultaneously, and it can be easily transformed to energy quantity and wind power curtailment cost. Another advantage is that the random planning problem can be converted to a deterministic one by calculating the expected values of functions which have several irrelevant random variables. These merits make the model not only to be able to consider the volatility of wind power, but also to avoid significantly increasing the difficulty in solving.

In addition, in order to coordinate new investment and wind power curtailment, per unit cost (i.e. social welfare loss, displacement cost of regular generators etc.) of wind power curtailment — C_{wind} is used in this paper to economically quantify the wind power output curtailment caused by an adjusted transmission plan.

Since discarding peak output saves transmission investment, the model aims to minimize the sum of transmission investment and cost of wind power curtailment [7], while satisfying system operation constraints. The objective function of the planning model is as shown in (2), where the two items represent investment in new lines and the expected cost of wind power curtailment respectively.

$$\min\left(\sum_{(i,j)\in\Omega} c_{ij}n_{ij} + C_{wind}\cdot\sum_{k=1}^{N_w}\left[t_k\cdot E\left(\Delta g_{wk}\right)\right]\right) \tag{2}$$

where c_{ij} is the cost of a line added to right-of-way $i-j$, and n_{ij} is the number of planned lines in right-of-way $i-j$. Ω is the set of all right-of-ways. C_{wind} is the cost of per MWh curtailment of wind energy. Δg_{wk} denotes the output curtailment of wind farm k. Meanwhile, N_w, k, and t_k represent the total number of wind farms, wind farm index, and the service life for wind farm k over the planning horizon, respectively. $E\left(\Delta g_{wk}\right)$ denotes the expected value of curtailed wind power per hour in wind farm k.

In reality, a system needs frequent and complex operation mode adjustments to deal with changes in some influencing factors [18], thus fairly affecting the amount of wind power curtailment. Therefore, it is necessary to consider the future operation uncertainties to enhance the adaptability of the planning scheme [19].

The multi-scenario method [17, 20] is applied to introduce operation uncertainties into the planning model. This method is usually used to handle the uncertainty which is difficult to be expressed mathematically [21]. In this paper, the future operation modes are described as a set of operation scenarios with corresponding probabilities of occurring.

Considering operation uncertainties, the objective function with multi-scenario is represented as follows:

$$\min\left\{\sum_{(i,j)\in\Omega} c_{ij}n_{ij} + C_{wind}\cdot\sum_{k=1}^{N_w} t_k\cdot\left\{\sum_{s=1}^{N_s} pr(s)\cdot E\left[\Delta g_{wk}(s)\right]\right\}\right\} \tag{3}$$

where s, N_s, $pr(s)$ and $\Delta g_{wk}(s)$ represent the scenario state variable, number of scenarios (uncertainties), the occurring probability of scenario s, and transmission-limited output of wind farm k in scenario s, respectively. The sum of $pr(s)$ equals to 1. $\sum_{s=1}^{N_s} pr(s)\cdot E\left[\Delta g_{wk}(s)\right]$ denotes the expected value of curtailed wind power per hour considering multi-scenario.

3.1.2 Operation and Planning Constraints:

The operation and planning constraints of this multi-scenario model include DC power flow constraints (4, 5), transmission capacity constraints in lines and transformers (6), generation output constraints (7, 8), the maximum number of line constraint (9), and integer constraint (10) [6, 22].

$$P_{ij}(s) - \frac{n_{ij}+n_{ij}^0(s)}{x_{ij}}\left(\theta_i(s)-\theta_j(s)\right) = 0 \tag{4}$$

$$\mathbf{M}^T\mathbf{P}_{\mathbf{L}}(s) + \mathbf{g}(s) + \mathbf{g}_{\mathbf{wm}}(s) = \mathbf{d}(s) \tag{5}$$

$$\left|P_{ij}(s)\right| \le \left(n_{ij}^0(s)+n_{ij}\right)\overline{P_{ij}} \tag{6}$$

$$\mathbf{g}_{\mathbf{min}}(s) \le \mathbf{g}(s) \le \mathbf{g}_{\mathbf{max}}(s) \tag{7}$$

$$0 \le \mathbf{g}_{\mathbf{wm}}(s) \le \mathbf{g}_{\mathbf{wc}} \tag{8}$$

$$0 \le n_{ij} \le \overline{n_{ij}} \tag{9}$$

$$n_{ij} \in \mathrm{N}^0 \tag{10}$$

where $n_{ij}^0(s)$, $\overline{n_{ij}}$, x_{ij}, and $P_{ij}(s)$ denote the number of lines in service in scenario s, the maximum number of lines that can be added, the reactance of a single line, and the power flow (all in right-of-way $i-j$) in scenario s. θ_i is the voltage phase angle of bus i. $\boldsymbol{M}^T$ is node-branch incidence matrix. $\mathbf{P}_{\mathbf{L}}(s)$ is the vector of $P_{ij}(s)$. $\boldsymbol{g}(s)$ represents the column vector of generator output in scenario s, and its maximum and minimum values are $\boldsymbol{g}_{max}$ and $\boldsymbol{g}_{min}$. $\mathbf{g}_{\mathbf{wm}}(s)$ is the vector of the upper limit of wind power output under the transmission plan in scenario s. It should be noted that $\mathbf{g}_{\mathbf{wm}}(s)$ is the objective function of the operation sub-problem that maximize wind power utilization in scenario s under current transmission plan, subject to operation constraints. The expected wind power curtailment in scenario s in the objective function (3) can be obtained through combining $\mathbf{g}_{\mathbf{wm}}(s)$ and the wind power output distribution curve. The upper limit of $\mathbf{g}_{\mathbf{wm}}(s)$ is its nominal capacity $\boldsymbol{g}_{wc}$. $\mathbf{d}(s)$ is load capacity in vector. $\overline{P_{ij}}$ is the maximum power flow of a single line in right-of-way $i-j$. N^0 is the set of non-negative integers.

3.1.3 Wind Output Curtailment Constraints:

As mentioned previously, full absorption of wind power

will lead to a huge transmission investment. On the other hand, due to the high investment, high operation and maintenance cost, the low annual utilization hours of wind power, the equivalent generation cost per kWh electricity of wind power is higher than that of conventional generation. Therefore, insufficient transmission will substantially increase the amount of abandoned wind power caused by transmission congestion, thus undermining the development and investment motivation of renewable energy. In order to enhance the applicability of the model, it is necessary to add flexible constraints to the planning result from two aspects: the overall wind energy utilization rate of the system and the utilization rate of wind energy in each wind farm.

From the perspective of overall wind energy utilization rate of the system, the whole amount of wind power output curtailment should be limited to an appropriate range. This constraint ensures the motivation for wind power investment and development. It can also guarantee that the final plan meets the commonly-used renewable energy development target "a certain percentage of total electricity comes from renewable energy". Therefore, the overall wind energy utilization rate constraint in the planning model is presented as follows, where γ is a given proportional coefficient in interval [0, 1].

$$\sum_{k=1}^{N_w} t_k \cdot \left\{ \sum_{s=1}^{N_s} pr(s) \cdot E\left[\Delta g_{wk}(s)\right] \right\} \le \gamma \cdot \sum_{k=1}^{N_w} t_k \cdot \left\{ \sum_{s=1}^{N_s} pr(s) \cdot E\left[g_{wk}(s)\right] \right\} \tag{11}$$

Constraint (11) represents that the sum of expected output curtailment of all wind farms should be less than a certain percentage of the total available wind energy, thus ensuring the overall utilization rate of wind energy.

Apart from the overall utilization rate, the wind energy utilization levels of some wind farms should also be considered in transmission planning. Therefore, another necessary constraint is presented as follows: where $\boldsymbol{\eta}$ is the vector of coefficients.

$$\boldsymbol{g}_{wm}(s) \ge \boldsymbol{\eta} \cdot \boldsymbol{g}_{wc} \tag{12}$$

Constraint (12) represents that the upper limit of wind power output for each wind farm in the transmission planning result is higher than a proportion of its nominal capacity in scenario *s*. This constraint ensures that wind power smaller than a given capacity in each wind farm can be transmitted to load without congestion, thus guaranteeing the wind energy utilization level of each wind farm in the final planning result. Since η is a vector-form parameter, the minimum wind energy utilization level of each wind farm can be separately controlled through this constraint.

The constraints (11) and (12), as well as their parameters γ and η, provide an approach to control the wind energy utilization levels in transmission planning, thus improving the applicability and flexibility of the model. For example, $\gamma = 0$ implies that there is no wind energy loss due to transmission constraints, which corresponds to full absorption of wind power. Obviously, if γ is set to 1 and η is set to 0, the two constraints do not work. The model containing (3) to (12) is condensed to the basic model containing (3) to (10), without any special consideration on wind energy utilization rates.

The objective function (3) and constraints (4)-(12) constitute a flexible multi-scenario transmission planning model that balances investment and wind energy loss. Since multi-scenario is introduced into the model, operation uncertainties can be easily considered. Each operation mode represented by a certain scenario has a specific constraints set $O_{st}(s)$. Therefore, multiple constraint sets which represent multiple scenarios can be considered simultaneously within the multi-scenario model, which could enhance the adaptability of the planning scheme. The advantages of the model are summarized as follows.

1) By setting different $\boldsymbol{g}_{min}(s)$ and $\boldsymbol{g}_{max}(s)$ in each scenarios, various typical operation modes can be considered in the model, such as "heavy-load scenario in wet seasons", "heavy-load scenario in dry seasons", etc.
2) By setting different $n_{ij}^0(s)$, which represents in-service or out-of-service states of important lines, the operation mode with key lines in maintenance can be considered in the model.
3) By setting different $\boldsymbol{d}(s)$, different forecasted load levels can be considered [21].
4) By combining different constants with operation state variables to form different sets of constraints, these obtained multiple complex scenarios can be considered simultaneously.
5) Since new scenarios can be easily introduced into the model as constraints set $O_{st}(s)$, the model possesses good flexibility and applicability.

3.2 The solution method based on probabilistic benders decomposition

Through Benders decomposition [21], this transmission planning problem can be decomposed into a planning master problem and an operation sub-problem. The master problem is solved to generate a trial solution for the planning decision variable, while the operation sub-problem is solved to generate Benders cuts, which are added to the master problem as constraints for the next iteration [23].

The solving process of the transmission planning model is given in Fig. 3. The details of the methodology are given below.

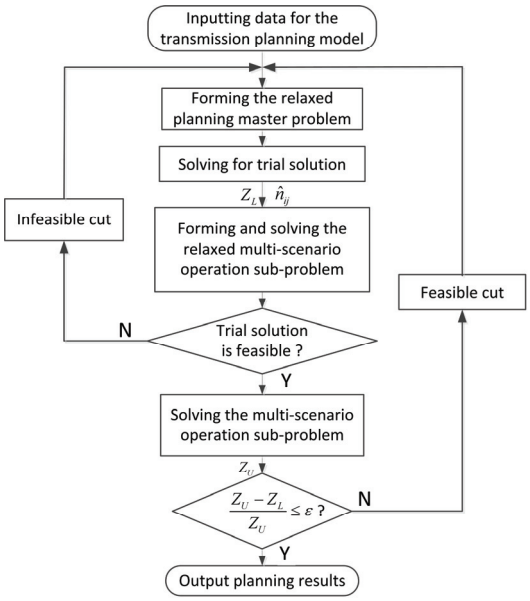

Fig. 3. The solving process of the panning problem by Benders decomposition

3.2.1 Planning Master Problem:

The master problem is an integer programming problem to determine the investment in lines, which only includes the constraints related to the decision variables. The master problem is given by

$$\min\ z \tag{13}$$

subject to the constraints (9), (10), and (14).

$$z \ge \sum_{(i,j)\in\Omega} c_{ij} n_{ij} \tag{14}$$

where z is a variable representing the master problem's objective.

This integer programming problem can be solved through the branch and bound method. After solving the master problem, a trial solution of n_{ij} and z in the master problem is obtained and denoted by $\hat{n}_{ij}$ and $\hat{z}$ respectively.

3.2.2 Relaxed Operation Sub-problem:

The objective of the relaxed operation sub-problem is set as the minimization of curtailment under all the operation constraints except the wind energy loss constraints (11) and the minimum wind power output space constraint (12). The objective function is as follows:

$$\min v = \sum_{k=1}^{N_w} t_k \cdot \left\{ \sum_{s=1}^{N_s} pr(s) \cdot E\left[\Delta g_{wk}(s)\right] \right\} \tag{15}$$

subject to constraints (5), (7), (8), (16), and (17).

$$P_{ij}(s) - \frac{\hat{n}_{ij} + n_{ij}^0(s)}{x_{ij}} \left(\theta_i(s) - \theta_j(s)\right) = 0 \tag{16}$$

$$\left|P_{ij}(s)\right| \le \left(n_{ij}^0(s) + \hat{n}_{ij}\right) \overline{P_{ij}} \tag{17}$$

The relaxed operation sub-problem is a non-linear constrained programming problem that can be solved through the interior-point method. After solving the relaxed operation sub-problem, the feasibility of its solution to the operation sub-problem is checked by the constraints (11) and (12). If the solution is infeasible, according to the solution of the relaxed operation sub-problem, dual variables of constraint set (16) and (17), constraint (11), and the theory of Benders decomposition [23], the infeasible cut is generated as follows:

$$\hat{v} + \sum_{(i,j)} \hat{\pi}_{ij} \cdot \overline{P_{ij}} (\hat{n}_{ij} - n_{ij}) \le \gamma \cdot \sum_{k=1}^{N_w} t_k \cdot \left\{ \sum_{s=1}^{N_s} pr(s) \cdot E\left[g_{wk}(s)\right] \right\} \tag{18}$$

where $\hat{v}$ and $\hat{\pi}_{ij}$ represent the objective value in (15) and the infeasible-cut multiplier, respectively.

3.2.3 Operation Sub-problem:

If the solution of the relaxed operation sub-problem satisfies (11) and (12), the operation sub-problem is solved, which is shown as follows:

$$\min\ w = C_{wind} \cdot \sum_{k=1}^{N_w} t_k \cdot \left\{ \sum_{s=1}^{N_s} pr(s) \cdot E\left[\Delta g_{wk}(s)\right] \right\} \tag{19}$$

subject to constraints (5), (7), (8), (11), (12), (16), and (17).

This non-linear programming problem can also be solved through the interior-point method. After solving the operation sub-problem, a feasible planning scheme and its objective value are obtained. If the convergence criterion is not satisfied, a feasible cut is generated as (20) to be added to the mater problem as a constraint. After that, one iteration step is completed [23].

$$z \ge \hat{w} + \sum_{(i,j)} \left(c_{ij} n_{ij} - \hat{\mu}_{ij} \cdot \overline{P_{ij}} (n_{ij} - \hat{n}_{ij}) \right) \tag{20}$$

where $\hat{w}$ and $\hat{\mu}_{ij}$ represent the objective value in (19) and the feasible-cut multiplier, respectively.

Convergence Criterion:

According to Benders decomposition [23, 24], the lower bound of the objective value is the objective value (13) in the master problem.

$$Z_L = \hat{z} \tag{21}$$

If the operation sub-problem is feasible, the upper bound of the original planning problem's objective value is given by

$$Z_U = \hat{z} + \hat{w} \tag{22}$$

The initial lower bound and upper bound are set as $-\infty$ and $+\infty$, respectively. As the iteration goes on, the gap between the two bounds gradually decreases. When they are close enough, the optimum solution of the original problem is obtained. Therefore, the convergence criterion is formulated as follows:

$$\left| \frac{Z_U - Z_L}{Z_U} \right| \leq \varepsilon \tag{23}$$

where ε is the predefined convergence boundary.

4. Case Study

4.1 Case description

The proposed approach is applied to a modified IEEE RTS-24 system [23], which has 10 generator buses, 17 load buses, 33 transmission lines, 5 transformers, and 33 generating units, without any wind power. Referring to the idea of [13], modifications of the system are as follows.

1) All the loads are increased to 1.5 times of their original values. All generation capacities (except the nuclear generators) are doubled. In addition, all lines' transmission capacities are reduced by 30%.
2) Bus 25 with 300MW and Bus 26 with 1200MW wind capacity are added, and they can be integrated into the system by the right-of-way 12-25, 13-25, 16-26, and 17-26.
3) All the existing 230kV right-of-ways are allowed to build new transmission lines, but the total numbers of lines on each right-of-way should be no more than three.
4) The construction cost of a 230kV and 138kV transmission line is 2×10^6\$/km and 1.5×10^6\$/km, respectively. The value of C_{wind} depends on many factors, such as the wind variable O&M cost, the cost of other generators providing displacement for curtail wind, actual system congestions, etc. For simplicity, C_{wind} is set to a fixed value — 30\$/MWh [25]. The planning horizon is 15 years and t_k s 15×8000h. η is set to 50%, which means that the final planning result should at least provide a grid-integration capacity which equals to half of the nominal capacity for each wind farm. The convergence error ε is 0.01. The initial value of γ is set to 0.01.

The modified 26-bus system includes 10 conventional generator buses, 2 wind power buses, 17 load buses, 38 transmission lines, and 21 right-of-ways. For simplicity in analysis, the maximum load of the planning horizon year (4275MW) is used as the load level in this case. The wind power output probability distribution is shown in Table 1.

Table 1. Discretized probability distribution of large-scale wind power output on bus 25 & 26

Wind power output (MW)		Probability
Bus 25	Bus 26	
0	0	0.050
20	120	0.080
60	240	0.150
90	360	0.300
120	480	0.245
150	600	0.120
180	720	0.034
210	840	0.010
240	960	0.006
270	1,080	0.003
300	1,200	0.002

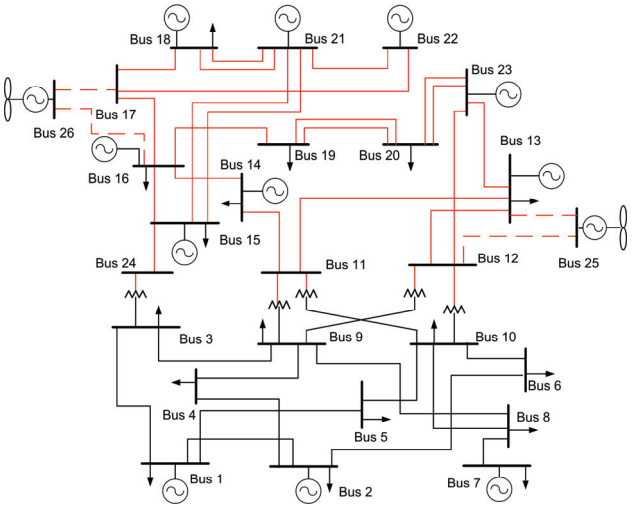

Fig. 4. Single line diagram of the modified IEEE-RTS

The single line diagram of the modified system is shown in Fig. 4.

The multi-scenario model is used in the study case to consider the uncertainties of generators and lines availability. For simplicity in analyzing, three scenarios with corresponding occurrence probabilities are considered in this study case: Scenario 1 (S1) denotes the heavy load operation mode in dry seasons, when hydro generation is sometimes in a low level to balance the system and the thermal generation covers most of the system load. Scenario 2 (S2) is the heavy load operation mode in wet seasons, in which hydro generation is always in a high level and the thermal generation sometimes decreases to balance the system. In Scenario 3 (S3), important lines ($n_{11,14}$, $n_{16,19}$) are in maintenance and other conditions are the same as S1.

4.2 Planning results

The probability of scenario S1, S2 and S3 are set to 0.5, 0.4, and 0.1, respectively. The multi-scenario model with peak output curtailment and the solving methodology based on Benders decomposition described in Section III

Table 2. Planning result

Planning scheme	Investment (1×106$)	Objective value (1×106$)	Expected curtailment of wind power
$n_{13,25}, n_{14,16} = 1$ $n_{16,26} = 3$	226.000	233.671	0.44%

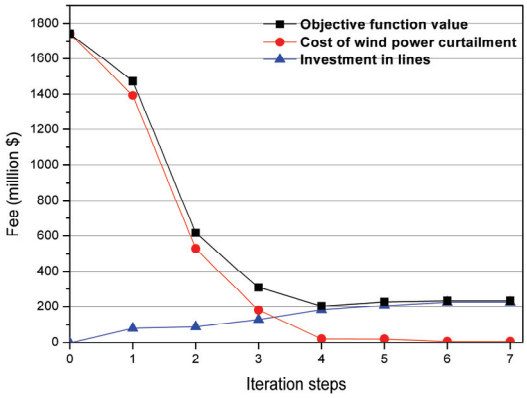

Fig. 5. The curves of objective function value, investment in lines, and cost of wind power curtailment in benders iterations

are applied to the case.

The program based on the proposed model and algorithm is performed on a desktop PC with 2.8 GHz Core2 E7300 CPU and 4□GB RAM. The total computation time is about 3.5 minutes. The planning result and the wind power curtailment information are shown in Table 2. The investments in lines, objective function values and costs of wind power curtailment during Benders iterations are given in Fig. 5.

Fig. 5 shows that in the early stage of the iterations, when investment increases, the cost of wind power curtailment decreases significantly, but the decrease slows down in the late stage of the iterations. This phenomenon is due to that in the late stage, the capacity of newly invested lines is mostly utilized by the peak output of wind power, which has a small probability of occurring. This phenomenon also indicates that curtailing a proper amount of peak output is reasonable and economic.

4.3 Performance analysis of different planning models

In order to investigate the characteristics of the proposed model through comparison, three symbols are used in the following analysis to denote the three planning models mentioned above, respectively:

- M_T — the traditional model without wind curtailment;
- M_C — the basic model with peak output curtailment;
- $M_{MS\text{-}C}$ — the multi-scenario model with peak output curtailment.

Combining the models (M_T, M_C, $M_{MS\text{-}C}$) and the scenarios (S1, S2, S3), five planning results are obtained and denoted by R1-R5, as shown in Table 3 and Table 4.

Table 3. Scenarios, planning models, and results

Scenario (Probability)	Model	γ	Planning result
S1 (1.0)	M_T	--	R1
S2 (1.0)	M_T	--	R2
S1 (1.0)	M_C	0.02	R3
S2 (1.0)	M_C	0.02	R4
S1 (0.6), S2 (0.4)	$M_{MS\text{-}C}$	0.02	R5

Table 4. Planning results R1-R5

Planning results	Planning scheme	Investment (1×106$)	Objective value (1×106$)
R1	$n_{13,25}, n_{14,16}, n_{17,26} = 1$ $n_{16,26} = 3$	292.000	292.000
R2	$n_{11,14}, n_{13,25}, n_{15,21} = 1$ $n_{16,17}, n_{16,19}, n_{17,26}$ $n_{14,16} = 2, n_{16,26} = 3$	540.000	540.000
R3	$n_{13,25} = 1, n_{16,26} = 2$	128.000	157.485
R4	$n_{13,25}, n_{14,16} = 1$ $n_{16,26} = 2$	182.000	202.808
R5	$n_{13,25}, n_{14,16} = 1$ $n_{16,26} = 2$	182.000	202.808

Table 5. Wind power curtailment information of R1-R4

Result-Scenario	Allowed maximum output of wind power		Total expected curtailment of wind power	
	Value (MW)	Percentage of nominal capacity	Value (MW)	Percentage of expected output
R1 in S1	1,500.0	100.0%	0.00	0.0%
R2 in S2	1,500.0	100.0%	0.00	0.0%
R3 in S1	956.2	63.7%	8.19	1.7%
R4 in S2	1000.0	66.7%	5.78	1.2%

4.3.1 Comparison of model M_T and M_C – Wind curtailment:

The planning results R1-R4 are analyzed to investigate the effects of wind curtailment on the model performance.

Table 5 gives the wind power curtailment information of planning results R1-R4. It shows that in scenario S1 and S2, the maximum wind power integration ability of the planning results given by MC (R3 and R4) are 36.3% and 33.3% respectively less than the nominal capacity. However, due to wind power output distribution characteristic, the expected curtailed output only accounts for 1.7% and 1.2% of the expected output over the planning horizon in S1 and S2, respectively. In other words, wind power curtailment reduces only a small proportion of the social welfare of total available wind energy.

In addition, it can be noticed from Table 4 that the investments of the plans given by M_C (R3 and R4) are 56.2% and 66.3% respectively less than those given by M_T (R1 and R2), due to that the curtailment of a proper amount of wind power reduce the required transmission capacity and saves investments in lines.

In summary, It can be noted that through considering the wind power output distribution characteristic to limit its output near to the rated capacity, transmission investment

is substantially reduced, while wind energy loss is relatively small. It shows that an appropriate output curtailment can obviously improve the economy of transmission expansion plans with an acceptable wind energy loss.

4.3.2 Comparison of model M_C and $M_{MS\text{-}C}$ – Multi-scenario:

For simplicity, the planning result R3 (given by M_C) and R5 (given by $M_{MS\text{-}C}$) in Table 4 are used to analyze the effects of multi-scenario on planning model performance. Table 6 shows the wind curtailment information of R3 and R5 in scenario S1 and S2.

It can be noted from Table 6 that in scenario S2, the allowed maximum wind power output of planning result R3 (given by M_C) is only 41.2% (less than the minimum 50% determined by η) of the nominal capacity. The expected curtailment reaches 23.4% (much more than the minimum 2% determined by γ) of all available wind energy.

Therefore, it can be seen that although the planning scheme given by M_C (R3) has a smaller investment, its amount of wind curtailment does not satisfy the curtailment constraints (10) and (11) in scenario S2. However, the planning scheme given by $M_{MS\text{-}C}$ (R5) can meet the curtailment constraints under S1 and S2, while still possessing considerable economic merits. In summary, compared with M_C, the planning model $M_{MS\text{-}C}$, which incorporates multi-scenarios, has better adaptability and can avoid additional investment in the future.

Table 6. Wind power curtailment information of R3 and R5

Result-Scenario	Allowed maximum output of wind power		Total expected output curtailment of wind power	
	Value (MW)	Percentage of nominal capacity	Value (MW)	Percentage of expected output
R3 in S1	956.2	63.7%	112.59	23.4%
R3 in S2	617.9	41.2%		
R5 in S1	700.0	58.3%	5.78	1.2%
R5 in S2	700.0	58.3%		

4.4 Sensitivity of the planning result to parameters in model $M_{MS\text{-}C}$

In the analysis above, C_{wind} is estimated to be 30$/MWh. It is necessary to take the variable characteristic of C_{wind} into account. Here, the value of C_{wind} is changed in order to analyze the sensitivity of the planning result to C_{wind}. The planning results given by $M_{MS\text{-}C}$ are shown in Table 7.

As shown in Table 7, when C_{wind} changes within the range of 30$/MWh to 90$/MWh, the planning scheme and the total investment are the same, while the cost of wind power curtailment varies slightly. This feature implies that the proposed method is not very sensitive to C_{wind}. Therefore, the planning model is still effective and applicable when the value of C_{wind} is not very precise or varies within a range over time.

Table 7. Planning result with different C_{wind} (γ=1)

C_{wind} ($/MWh)	Planning scheme	Investment (1×106$)	Objective value (1×106$)
30	$n_{13,25}, n_{14,16}=1, n_{16,26}=3$	226.000	233.671
60	$n_{13,25}, n_{14,16}=1, n_{16,26}=3$	226.000	241.342
90	$n_{13,25}, n_{14,16}=1, n_{16,26}=3$	226.000	249.013

Table 8. Planning result with different γ

γ	Planning scheme	Investment (1×106$)	Objective value (1×106$)
0.0250	$n_{13,25}, n_{14,16}=1, n_{16,26}=2$	182.000	204.127
0.0200	$n_{13,25}, n_{14,16}=1, n_{16,26}=2$	182.000	204.127
0.0150	$n_{13,25}, n_{14,16}=1, n_{16,26}=2$	182.000	204.127
0.0125	$n_{13,25}, n_{14,16}=1, n_{16,26}=3$	226.000	233.671
0.0050	$n_{13,25}, n_{14,16}=1, n_{16,26}=3$	226.000	233.671
0.0025	$n_{13,25}, n_{14,16}, n_{15,16}, n_{16,19}=1$ $n_{16,26}=3$	258.000	260.899
0.0000	$n_{11,14}, n_{13,25}, n_{16,17}=1$ $n_{16,19}, n_{15,21}, n_{17,26}$ $n_{14,16}=2, n_{16,26}=3$	540.000	540.000

In order to test the sensitivity to γ, γ is set to 0.0250, 0.0200, 0.0150, 0.0125, 0.0050, 0.0025, and 0.0000 in $M_{MS\text{-}C}$, Obtained planning schemes are shown in Table 8.

As shown in Table 8, the investment in lines increases as γ decreases, but the relationship is not continuous since the numbers of lines are integers. Only when γ decreases by a certain amount, is a new line added to the planning scheme, thus increasing the investment stepwise accordingly.

Fig. 6 shows that as γ decreases, the increase of investment in new lines is much faster than the decrease of the cost of wind power curtailment, and huge transmission investment is needed for full ($\gamma=0$) or nearly-full (γ<0.0025) absorption of wind power. For instance, if γ changes from 0.0050 to 0.0025, investment increases by $32\times10^6$$ while the cost of wind power curtailment only decreases by $4.772\times10^6$$, which is a very low return for transmission investments increase. Even if assuming that the cost of wind power curtailment per MWh is 4 times larger than the original value, the return on investment increase is still low. Therefore, in order to obtain the optimal planning result, the appropriate range for γ is [0.005, 0.0125]. This means allowing about 1 percent of total wind energy to be curtailed in transmission planning.

Since the proposed model can significantly increase social welfare through sacrificing a small fraction of wind energy, the optimal planning result may lead to a slight reduction on the electricity generated by wind farms, which is related to the revenues of wind farms. The potential revenue loss of wind farms can be compensated through a compensation system, whose specific implementation methods can be formulated according to actual situations.

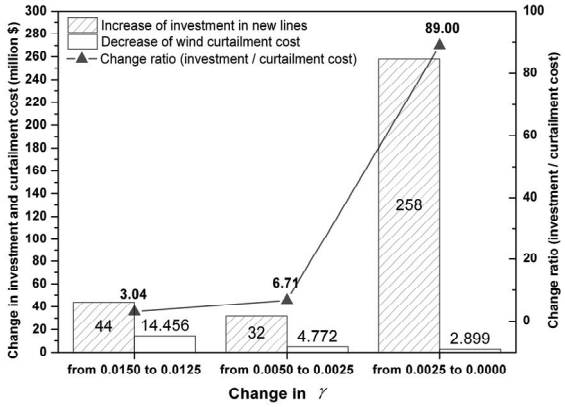

Fig. 6. The change in investment and cost of wind power curtailment due to the change in γ

5. Conclusion

Through analyzing the wind power output distribution characteristics of wind power output and its effects on transmission planning, it is demonstrated that in order to generate a more economic expansion planning for integrating large-scale wind power, utilization of wind energy and investment in lines should be all taken into consideration. Both full absorption of wind power policy and the wind output being curtailed inappropriately with inadequate transmission would lead to uneconomic expansion planning. Incorporating the cost of wind power curtailment into the planning model can make the expansion planning more economical. Furthermore, the introduction of multi-scenarios makes the model more flexible and adaptable to future operation uncertainties. The results show that the solving methodology based on Benders decomposition can solve the problem effectively. In summary, this new planning model and its solving method provide an economic way of transmission expansion planning for large-scale wind power integration.

Acknowledgements

This work has been supported by the National Natural Science Foundation of China under Grant 51277141 and the National High Technology Research and Development Program of China (863 Program) under Grant 2011 AA05A103. Three reviewers are acknowledged for their comments on an earlier version of this manuscript.

References

[1] M. Yao, and L. Yao, "Integration of large scale wind farm into electrical grids," *Proc. China Int. Conf. on Electricity Distribution* (*CICED*), pp. 1-5, 13-16 Sep. 2010.

[2] Jae Hyung Roh, Mohammad Shahidehpour, and Lei Wu, "Market-based generation and transmission planning with uncertainties," *IEEE Trans. Power Systems*, vol. 24, no. 3, pp. 1587-1598, 2009.

[3] Guk-Hyun Moon, Seong-Bae Kong, Sung-Kwan Joo, et al., "Stochastic Integrated Generation and Transmission Planning Incorporating Electric Vehicle Deployment," *Journal of Electrical Engineering & Technology*, vol. 8, no. 1, pp. 1-10, 2013.

[4] Gerardo Latorre, Rubén Darío Cruz, Jorge Mauricio Areiza, et al., "Classification of publications and models on transmission expansion planning," *IEEE Trans. Power Systems*, vol.18, no.2, pp.938-946, 2003.

[5] Gholam-Reza Kamyab, Mahmood Fotuhi-Firuzabad, and Masoud Rashidinejad, "Market-Based Transmission Expansion Planning Under Uncertainty in Bids by Fuzzy Assessment," *Journal of Electrical Engineering & Technology*, vol. 16, pp. 18, 2012.

[6] R. Romero, A. Monticelli, A. Garcia, et al., "Test systems and mathematical models for transmission network expansion planning," *Proc. Inst. Elect. Eng., Gen.*, Transm*., Distrib.*, vol. 149, no. 1, pp. 27-36, Jan. 2002.

[7] J. Choi, T. D. Mount, R. J. Thomas, et al., "Probabilistic reliability criterion for planning transmission system expansions," *Proc. Inst. Elect. Eng., Gen., Transm., Distrib.*, vol.153, no.6, pp.719-727, Nov. 2006.

[8] R. Karki, P. Hu, and R. Billinton, "Adequacy criteria and methods for wind power transmission planning, " *Power & Energy Society General Meeting, PES. IEEE*, pp. 1-7, 26-30 July 2009.

[9] E. Denny, and M. O'Malley, "Quantifying the total net benefits of grid integrated wind," *IEEE Trans. Power Systems*, vol.22, no.2, pp. 605-615, May 2007.

[10] J. F. Restrepo, and F. D. Galiana, "Assessing the yearly impact of wind power through a new hybrid deterministic/stochastic unit commitment," *IEEE Trans. Power Systems*, vol. 26, no. 1, pp. 401-410, Feb. 2011.

[11] J. Kabouris, and C. D. Vournas, "Application of interruptible contracts to increase wind-power penetration in congested areas," *IEEE Trans. Power Systems*, vol. 19, no. 3, pp. 1642-1649, Aug. 2004.

[12] D. Villanueva, J.L. Pazos, and A. Feijoo, "Probabilistic load flow including wind power generation," *IEEE Trans. Power Systems*, vol. 26, no. 3, pp. 1659-1667, Aug. 2011.

[13] R. Billinton, and W. Wangdee, "Reliability-based transmission reinforcement planning associated with large-scale wind farms," *IEEE Trans. Power Systems*, vol. 22, no. 1, pp. 34-41, Feb. 2007.

[14] J. Ge, M. Du, and C Zhang, "A study on correlation of wind farms output in the large-scale wind power base, " *Proc. 4th Int. Electric Utility Deregulation and Restructuring and Power Technologies (DRPT) Conf.*, pp. 1316-1319, 6-9 July 2011.

[15] R. Karki, Hu Po, and R. Billinton, "A simplified wind power generation model for reliability evaluation,"

IEEE Trans. Energy Conversion, vol. 21, no. 2, pp. 533-540, June 2006.
[16] M. Nick, GH Riahy, SH Hosseinian, et al., "Wind power optimal capacity allocation to remote areas taking into account transmission connection requirements," *IET Renew.* Power *Gener.*, vol. 5, no. 5, pp. 347-355, Sep. 2011.
[17] B. G. Gorenstin, N. M. Campodonico, J. P. Costa, et al., "Power system expansion planning under uncertainty," *IEEE Trans. Power Systems*, vol. 8, no. 1, pp. 129-136, Feb. 1993.
[18] P. Sanchez-Martin, A. Ramos, and J. F. Alonso, "Probabilistic midterm transmission planning in a liberalized market," *IEEE Trans. Power Systems*, vol. 20, no. 4, pp. 2135-2142, Nov. 2005.
[19] J. T. Saraiva, V. Miranda, and L. M. V. G. Pinto, "Impact on some planning decisions from a fuzzy modelling of power systems," *IEEE Trans. Power Systems*, vol. 9, no. 2, pp. 819-825, May 1994.
[20] V. Miranda, and L. M. Proenca, "Probabilistic choice vs. risk analysis-conflicts and synthesis in power system planning," *20th Int.* Conf. *on Power Industry Computer Applications*, pp. 16-21, 11-16 May 1997.
[21] F. S. Reis, P. M. S. Carvalho, and L. A. F. M. Ferreira, "Reinforcement scheduling convergence in power systems transmission planning," *IEEE Trans. Power Systems*, vol. 20, no. 2, pp. 1151-1157, May 2005.
[22] I. de J Silva, M. J. Rider, R. Romero, et al., "Transmission network expansion planning with security constraints," *Proc. Inst. Elect. Eng., Gen., Transm., Distrib.*, vol. 152, no. 6, pp. 828-836, Nov. 2005.
[23] MKC Marwali, and SM Shahidehpour, "Integrated generation and transmission maintenance scheduling with network constraints," *IEEE Trans. Power Systems*, vol. 13, no. 3, pp. 1063-1068, Aug. 1998.
[24] S. Binato, M.V.F. Pereira, and S. Granville, "A new Benders decomposition approach to solve power transmission network design problems," *IEEE Trans. Power Systems*, vol.16, no.2, pp. 235-240, May 2001.
[25] Lingfeng Wang, and Chanan Singh, "Balancing risk and cost in fuzzy economic dispatch including wind power penetration based on particle swarm optimization," *Electric Power Systems Research*, vol. 78, no. 8, pp. 1361-1368, 2008.

Jianxue Wang He received the B.S. M.S. and Ph.D. degree from Xi'an Jiaotong University, Xi'an, China, all in electrical engineering, in 1999, 2002 and 2006 respectively. He is the Associate Professor at the Department of Electrical Engineering of Xi'an Jiaotong University from 2008. His research interests include the renewable energy and microgird.

Ruogu Wang He received his B.S. and M.S. degrees in electrical engineering from Xi'an Jiaotong University, Xi'an, China, in 2006 and 2012 respectively. From 2012, he has been with Shaanxi Electric Power Research Institute as an electrical engineer. His major research interests are renewable energy, power system planning and operation.

Pingliang Zeng He received his B.S. degree in 1984 from Huazhong University of Science and Technology, Wuhan, China, and Ph.D. degree in 1990 from Strathclyde University, Glasgow, UK, both in electrical engineering. From 1990 to 2012, he worked in National Grid Company, UK. He is currently with China Electrical Power Research Institute in Beijing, China, as the Chief Expert in Power System Analysis and Planning. His main research interests include power system planning and electricity market.

Shutang You He received his B.S. and M.S. degrees in electrical engineering from Xi'an Jiaotong University, Xi'an, China, in 2011 and 2014 respectively. He is currently pursuing his Ph.D. degree at University of Tennessee-Knoxville, Knoxville, USA. His major research interests include power system reliability and renewable energy.

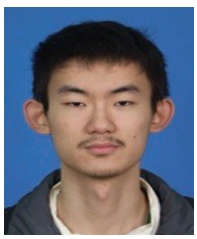

Yunhao Li He received the B.S. in electrical engineering from Huazhong University of Science and Technology in 2012. He is currently pursuing the Ph.D. degree at Xi'an Jiaotong University. His research interests include renewable energy and power system planning.

Yao Zhang He received the B.S. and M.S. degrees from Xi'an Jiaotong University, Xi'an, China, all in electrical engineering, in 2010 and 2013 respectively. He is currently pursuing the Ph.D. degree at Xi'an Jiaotong University. His research interests include probabilistic energy forecasting and stochastic optimization under uncertainty.